

Effective Tuning of HOMO and LUMO Energy Levels by $p-n$ Diblock and Triblock Oligomer Approaches

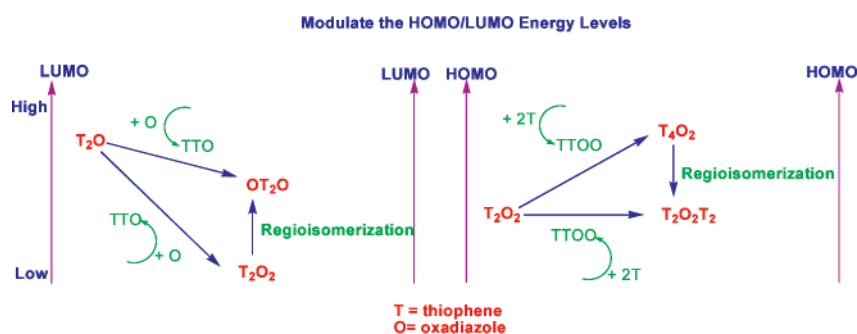
Jun-Hua Wan,[†] Jia-Chun Feng,[†] Gui-An Wen,[†] Wei Wei,[†] Qu-Li Fan,[†] Chuan-Ming Wang,[†] Hong-Yu Wang,[†] Rui Zhu,[†] Xiang-Dong Yuan,[†] Chun-Hui Huang,[†] and Wei Huang^{*,†,‡,§}

Institute of Advanced Materials (IAM), Fudan University, Shanghai 200433, China, Institute of Advanced Materials (IAM), Nanjing University, Nanjing 210093, China, and Department of Chemical and Biomolecular Engineering, National University of Singapore, 10 Kent Ridge Crescent, Singapore 119260, Republic of Singapore

wei-huang@fudan.edu.cn; chehw@nus.edu.sg

Received October 17, 2005

This paper was withdrawn by the Editor on August 25, 2006 (*J. Org. Chem.* 2006, 71, 7124).



A novel series of oligomers consisting of thiophene as a p -type unit and oxadiazole as an n -type unit were separately synthesized. On the basis of the characterization of photophysical and electrochemical properties, the structure–property relationships of the oligomers were investigated. Cyclic voltammogram studies showed that changing the number of thiophene and oxadiazole units could effectively modulate the electronic properties of the $p-n$ diblock and triblock oligomers. The effect of molecular regiochemistry on electronic properties is also investigated. The observed electronic properties were consistent with theoretical calculations. These systems serve as excellent examples, demonstrating the band gap control principle in the $p-n$ heterostructure oligomers.

Introduction

π -Conjugated thiophene-based polymers and oligomers have been investigated extensively in the past decade because of their potential applications in semiconductor devices such as thin film organic field-effect transistors,¹ organic light-emitting diodes,² photovoltaic cells,³ and molecular rectifiers.⁴ Most of these applications would benefit from a full understanding of charge-transport properties, which depend on the morphology of thin films and the electronic structures.⁵ Therefore, developing a methodology to modulate the HOMO and LUMO energy levels of the elemental conjugated units is indispensable. In our previous work, we have developed the $p-n$ diblock concept

and obtained several series of $p-n$ diblock conjugated polymers.⁶ The variation of the length of the p and n segments in the block polymer chain afforded the possibility of tuning the HOMO and LUMO energy levels and emissive wavelength. These polymers show improved photoluminescent and elec-

* To whom correspondence should be addressed. Tel: +86 21 5566 4188/4198. Fax: +86 21 6565 5123/5566 4192.

[†] Fudan University.

[‡] Nanjing University.

[§] National University of Singapore.

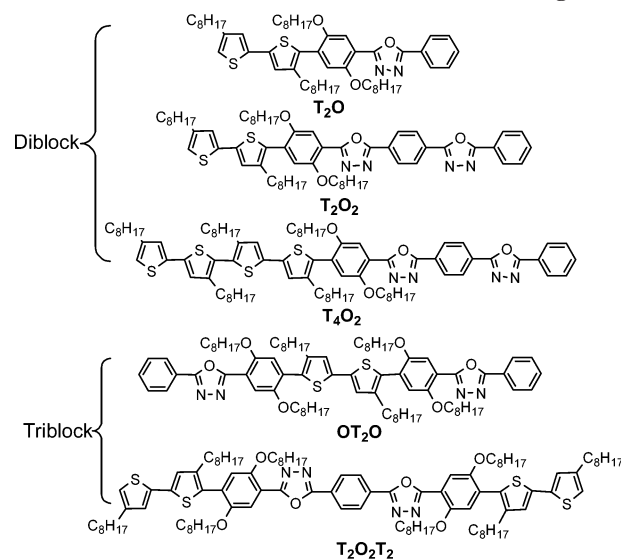
(1) (a) Dimitrakopoulos, C. D.; Malenfant, R. L. *Adv. Mater.* **2002**, *14*, 99. (b) Pappenfus, T. M.; Chesterfield, R. J.; Frisbie, C. D.; Mann, K. R.; Casado, J.; Raff, J. D.; Miller, L. L. *J. Am. Chem. Soc.* **2002**, *124*, 4184. (c) Katz, H. E.; Bao, Z. N.; Gilat, S. L. *Acc. Chem. Res.* **2001**, *34*, 359. (d) Heeney, M.; Bailay, C.; Genevicius, K.; Shkunov, M.; Sparrowe, D.; Tierney, S.; McCulloch, I. *J. Am. Chem. Soc.* **2005**, *127*, 1078. (e) Horowitz, G. *Adv. Mater.* **1998**, *10*, 3. (g) Garnier, F. *Acc. Chem. Res.* **1999**, *32*, 209. (h) Rogers, J. A.; Bao, Z.; Dodabalapur, A.; Grone, B.; Raju, V. R.; Katz, H. E.; Kuck, V.; Amundson, k. J.; Drzaic, P. *Proc. Natl. Acad. Sci. U.S.A.* **2001**, *98*, 4817.

(2) (a) Mitschke, U.; Bauerle, P. *J. Mater. Chem.* **2000**, *10*, 1471. (b) Barbarella, G.; Melucci, M.; Sotgiu, G. *Adv. Mater.* **2005**, *17*, 1581 and references therein. (c) Barbarella, G.; Favaretto, L.; Zambianchi, M.; Pudova, O.; Arbizzani, C.; Bongini, A.; Mastragostino, M. *Adv. Mater.* **1998**, *10*, 551. (d) Noda, T.; Shirota, Y. *J. Am. Chem. Soc.* **1998**, *120*, 9714.

roluminescent properties. However, the improvement is still lower than the expected level. The poor improvement may be attributed to the alternating distribution of the *p* segment and *n* segment in the polymer chain. The electron deficient unit inserted into the *p*-type polymer chain will partially act as the hole-blocking unit as a result of its high electron deficiency. Conversely, the hole-transporting unit will lower the electron mobility.

Actually, the above-mentioned drawback can be resolved by the diblock oligomer that has two separate blocks, which is consistent with the *p*-type and *n*-type units, respectively. The *p*-*n* diblock oligomer,⁷ which is an idea analogous to the semiconductor *p*-*n* junction, combined easy charge injection with current rectification properties. Additionally, in comparison with the conjugated copolymers, the monodisperse conjugated oligomers, possessing well-defined conjugation lengths and structures, are characterized by structural uniformity, ease of purification, and characterization.⁸ Furthermore, deep electron traps possibly occur in polymeric systems as a result of chain entanglements or structural defects.⁹ Recently, a thiophene–thiazole diblock oligomer has been synthesized, and the rectification properties have been investigated in a molecular rectifier device.⁴ However, the report about the systematic study for the electronic properties of the *p*-*n* diblock system is still lacking. No general concept for the *p*-*n* diblock oligomer system has been established as yet. In this article, a novel series of diblock oligomers (**T₂O**, **T₂O₂**, **T₄O₂**), consisting of an electron-rich thiophene unit and an electron-deficient oxadiazole unit with different unit lengths, are successfully synthesized. Furthermore, the electronic properties of these oligomers are investigated systematically. For the investigation of the effect of molecular regiochemistry on the electrochemical and optical

SCHEME 1. Structures of Diblock and Triblock Oligomers



properties, another series of *n*-*p*-*n* (**OT₂O**) and *p*-*n*-*p* (**T₂O₂T₂**) triblock oligomers were also synthesized (Scheme 1).

Results and Discussion

Synthesis and Characterization. Generally, the oligomer syntheses involve three procedures, that is, the synthesis of the oxadiazole monomers, the synthesis of the thiophene monomers, and the coupling reaction.

Schemes 2 and 3 show the synthetic routes of the oxadiazole monomers. The common synthetic sequence of 4-bromo-2,5-bis(octyloxy)benzoic acid methyl ester **2** involves three steps,¹⁰ which is too complicated (Scheme 2). We developed a one-pot synthetic route for compound **2** from 1,4-dibromo-bis(octyloxy)benzene **1**. Compound **2** with 60% yield is prepared by treating **1** with *n*-BuLi and treated further with liquid dimethyl carbonate, which was used more conveniently than gaseous CO₂. Moreover, the monobromo-substituted oxadiazole dimer was synthesized successfully (Scheme 3). To the best of our knowledge, no monobromo-substituted oxadiazole dimer has been synthesized as yet. To obtain compound **8**, the mixture of compound **3** and benzohydrazide in pyridine is added into the solution of terephthaloyl dichloride in anhydrous THF slowly by syringe. Compound **8** was obtained with 45% yield after the two byproducts were removed by silica gel chromatography. After cyclodehydration of compound **8**, monobromo-substituted oxadiazole dimer **9** was obtained with 73% yield.

The synthesis of the thiophene monomers **13** and **14** are depicted in Scheme 3. After crystallizing from ether at -78 °C, 4,4'-dioctyl-2,2'-bithiophene was obtained with 70% yield from 3-octylthiophene by the oxidative coupling of the lithiated derivative in the presence of copper chloride. The *n*-BuLi/Bu₃SnCl sequence carried out on monobromo and dibromo derivatives, obtained by the reaction of **1** and **2** equiv of NBS on compound **10** in CHCl₃/HOAc (1:1), lead to the stannanes **13** and **14**. The stannanes **13** and **14** were used without further purification as a result of their decomposition on silica gel.

Scheme 4 shows the synthetic route to the oligomers. The oligomers are obtained with moderate yield through the coupling

(3) (a) Vidélot, C.; Kassmi, A. Z.; Fichou, D. *Sol. Energy Mat. Sol. Cells* **2000**, *63*, 69. (b) Bettingnies, R. D.; Nicolas, Y.; Blanchard, P.; Levillain, E.; Nunzi, J.-M.; Roncali, J. *Adv. Mater.* **2003**, *15*, 1939. (c) Liu, J.; Kadnikova, E. N.; Liu, Y.; McGehee, M. D.; Frechet, J. M. J. *J. Am. Chem. Soc.* **2004**, *126*, 9486. (d) Campos, L. M.; Tontcheva, A.; Gunes, S.; Sonmez, G.; Neugebauer, H.; Sariciftci, N. S.; Wudl, F. *Chem. Mater.* **2005**, *17*, 4031.

(4) (a) Ng, M.-K.; Lee, D.-C.; Yu, L. P. *J. Am. Chem. Soc.* **2002**, *124*, 11862. (b) Jiang, P.; Morales, G. M.; You, W.; Yu, L. P. *Angew. Chem., Int. Ed.* **2004**, *43*, 4471.

(5) (a) Facchetti, A.; Yoon, M.-H.; Sten, C. L.; Katz, H. Z.; Mark, T. J. *Angew. Chem., Int. Ed.* **2003**, *42*, 3900. (b) Turbiez, M.; Frere, P.; Allain, M.; Vidélot, C.; Ackermann, J.; Roncali, J. *Chem.—Eur. J.* **2005**, *11*, 3472. (c) Kiriy, N.; Bocharova, V.; Kiriy, A.; Stamm, M.; Krebs, F. C.; Adler, H.-J. *Chem. Mater.* **2004**, *16*, 4765.

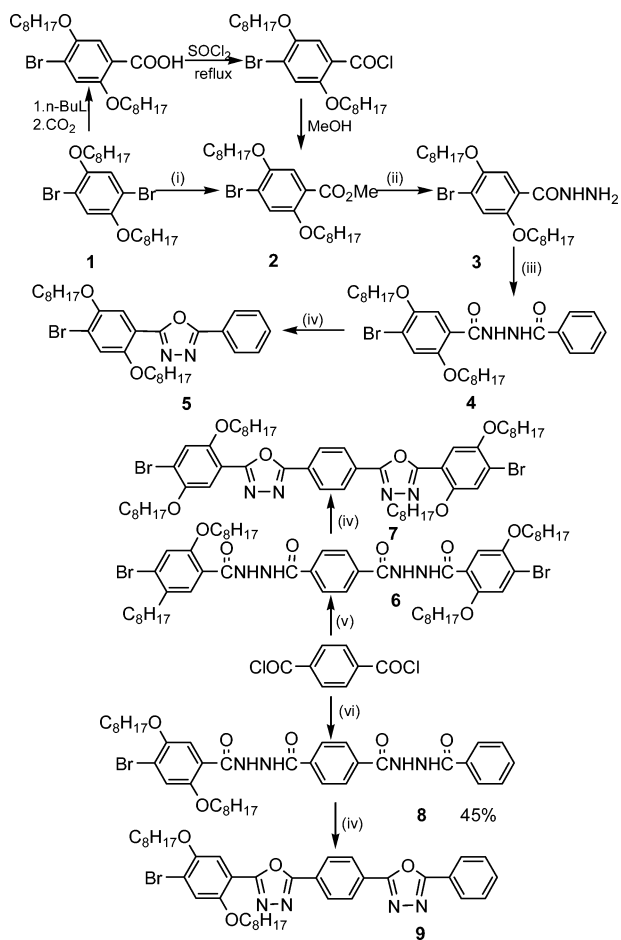
(6) Yu, W.-L.; Meng, H.; Pei, J.; Huang, W. *J. Am. Chem. Soc.* **1998**, *120*, 11808.

(7) In normal polymer concepts, the term “block polymer” means “the polymer with several blocks that contain a large number of repeating units”. The most common block polymers are the diblock and triblock polymers, represented by A_nB_m and A_nB_mA_n or A₁B₁C₁ (A, B, and C represent different repeating units), respectively. However, the polymer with the structure ... ABABAB ... is named an alternating copolymer instead of a block polymer. Also, the term “oligomer” means “the polymer with less repeating units and a low molecular weight compared with that of a common polymer”. In our manuscript, we introduced the terms “diblock oligomer” and “triblock oligomer” because they possess the same structure as the diblock and triblock polymers. The difference is the block length of the oligomer is much less than that of a polymer. For example, the oligomers with the AAABBB and AAABBBAAA structures can be named diblock and triblock oligomers, respectively. In addition, the *p*-type unit and *n*-type unit refer to the electron-rich segment and electron-deficient segment, respectively.

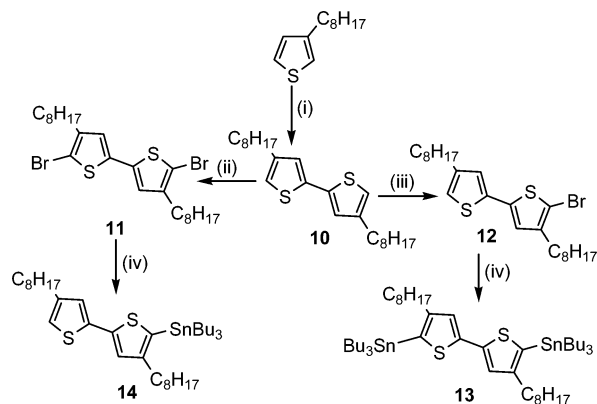
(8) (a) Klubek, K.; Vaeth, K. M.; Tang, C. W. *Chem. Mater.* **2003**, *15*, 4352. (b) Lee, S.-H.; Nakamura, T.; Tsutsui, T. *Org. Lett.* **2001**, *3*, 2005. (c) Pei, J.; Wang, J.-L.; Cao, X.-Y.; Zhou, X.-H.; Zhang, W.-B. *J. Am. Chem. Soc.* **2003**, *125*, 9944.

(9) Wu, C.-C.; Liu, T.-L.; Hung, W.-Y.; Lin, Y.-T.; Wong, K.-T.; Chen, R.-T.; Chen, Y.-M.; Chien, Y.-Y. *J. Am. Chem. Soc.* **2003**, *125*, 3710.

(10) Ding, J.; Day, M.; Robertson, G.; Roovers, J. *Macromolecules* **2002**, *35*, 3474.

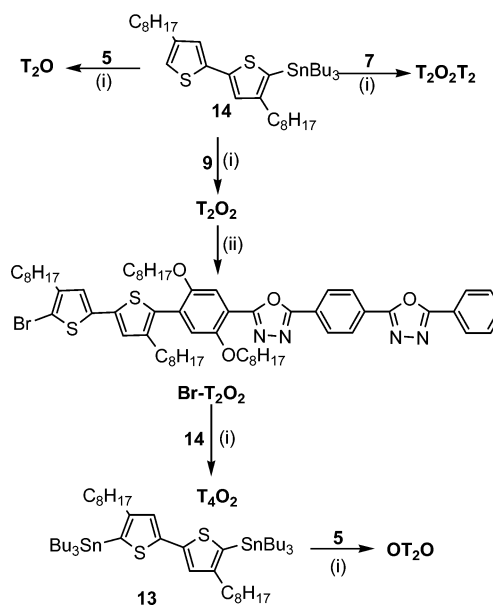
SCHEME 2^a

^a Reaction conditions: (i) *n*-BuLi, -78 °C, Me_2CO_3 , THF; (ii) $\text{NH}_2\text{NH}_2 \cdot \text{H}_2\text{O}$, MeOH; (iii) benzoyl chloride, pyridine; (iv) POCl_3 , 80 °C; (v) **3**, pyridine; (vi) the solution of **3** and benzohydrazide in pyridine, THF.

SCHEME 3^a

^a Reaction conditions: (i) *n*-BuLi/TMEDA, CuCl_2 ; (ii) 2.0 equiv NBS, $\text{CHCl}_3/\text{HOAc}$; (iii) 1.0 equiv NBS, $\text{CHCl}_3/\text{HOAc}$; (iv) *n*-BuLi, Bu_3SnCl .

of the thiophene monomers and the corresponding oxadiazole monomers by Stille reaction. As a result of the difficulty in obtaining the pure monobromo-substituted tetrathiophene monomer through the ordinary route, **T₄O₂** was obtained through a Stille coupling reaction of the stannane **14** with compound **Br-T₂O₂**, which was afforded by the bromination of **T₂O₂** with NBS.

SCHEME 4^a

^a Reaction conditions: (i) $\text{Pd}(\text{PPh}_3)_4$, 3%, 100 °C, toluene; (ii) NBS, $\text{CHCl}_3/\text{AcOH}$.

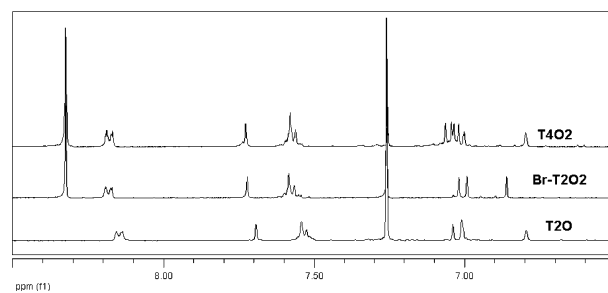


FIGURE 1. ¹H NMR spectra in the aromatic range for oligomers.

The structure and purity of the oligomers were verified by ¹H and ¹³C NMR, MALDI-TOF MS, and elemental analysis. For all oligomers, the two triplet signals on the ¹H NMR spectra arising from between δ 4.00 and 4.11 ppm belong to the protons of the first methylene at the 3-position of the thiophene rings. The single signal arising from about δ 6.86 ppm originates from the proton neighboring the thiophene ring of the 1,4-bis-(octyloxy)benzene ring in the oligomers. Therefore, it is easy to identify the oligomers through the relative integration of these characteristic signals in the ¹H NMR spectra. In the ¹H NMR spectra of **Br-T₂O₂**, the signal arising from δ 7.03 ppm disappears, which was assigned to the α proton of the terminal thiophene ring of **T₂O₂** (Figure 1). It is convenient to monitor the brominating process through the change of this characteristic signal in the ¹H NMR spectra.

Optical Properties. Spectroscopic properties of the oligomers were investigated with UV-vis absorption and fluorescence emission. Figure 2a shows the absorption spectra of the oligomers in toluene solutions. The oligomers, **T₂O₂**, **T₄O₂**, and **T₂O₂T₂**, show two distinct absorption bands. The absorption bands in the longer wavelength range (above 360 nm) come from the thiophene units,¹¹ and the remarkable enhancement of the absorption intensity in **T₄O₂** relative to **T₂O₂** reflects the

(11) Chen, S. Y.; Liu, Y. Q.; Qiu, W. F.; Sun, X. B.; Ma, Y. Q.; Zhu, D. B. *Chem. Mater.* **2005**, *17*, 2208.

TABLE 1. Optical Properties of the Oligomers

oligomer	$\lambda_{\text{max, abs}}$ (nm)			$\lambda_{\text{max, em}}$ (nm)			E_g^c (eV)
	toluene ^a	CH ₂ Cl ₂ ^a	film ^b	toluene ^a	CH ₂ Cl ₂ ^a	film ^b	
T ₂ O	362	363	372	441	449	470	2.98
T ₂ O ₂	312/373	312/373	319/405	446	464	498	2.90
T ₄ O ₂	314/377	316/381	319/394	495	508	524	2.77
OT ₂ O	376	378	397	471	476	492	2.86
T ₂ O ₂ T ₂	315/376	294/377	320/393	451	471	483	2.91

^a Measured in solution (1×10^{-5} M). ^b Measured in solid thin film on quartz plates prepared by spin coating from solution. ^c Optical band gap derived from the onset of UV-vis absorption spectra of oligomer solutions.

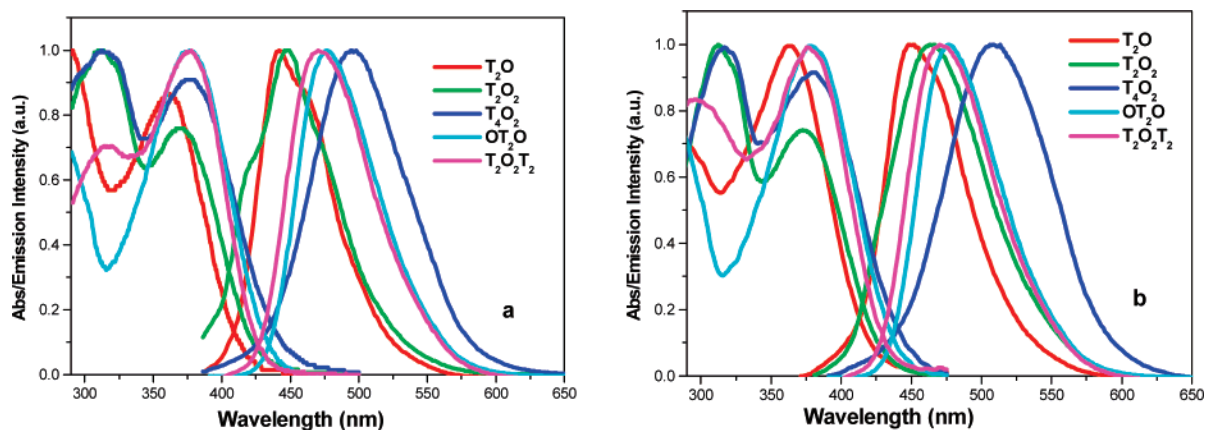


FIGURE 2. Absorption and fluorescence spectra for oligomers (a) in toluene solution and (b) in CH₂Cl₂ solution, respectively.

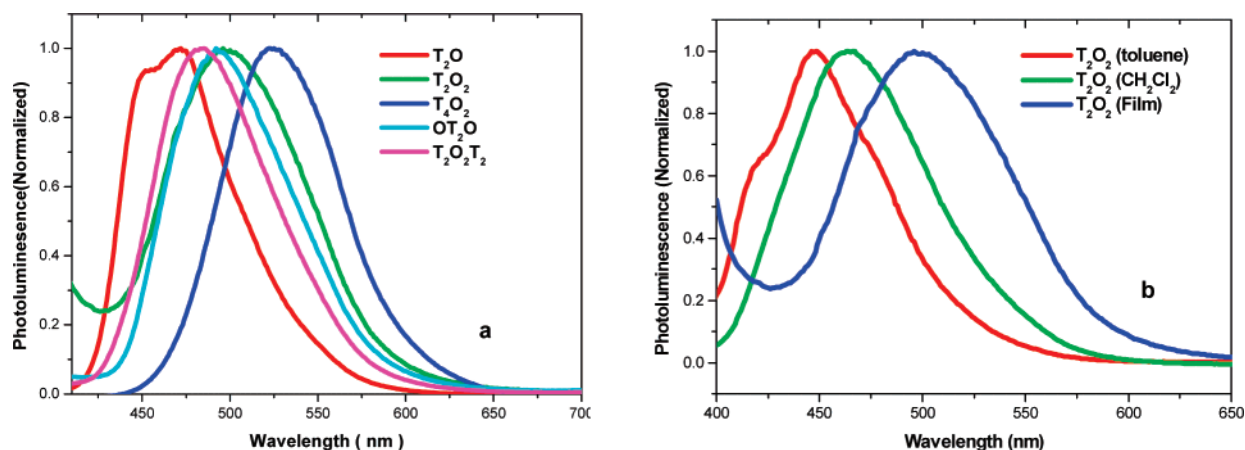


FIGURE 3. Fluorescence spectra for oligomers (a) in solid thin film and (b) for T₂O₂ in different environments, respectively.

corresponding increases in the number of thiophene units in the oligomers. Other absorption bands of T₂O₂, T₄O₂, and T₂O₂T₂ (around 300 nm) come from the $\pi-\pi^*$ transition of the oxadiazole groups.¹² This implies that the electronic interactions between the oxadiazole units and the thiophene units are rather limited in their ground states.⁹ Nevertheless, both T₂O and OT₂O display no remarkable absorption bands in the shorter wavelength range.

The absorption spectra of the oligomers in the polar solvent CH₂Cl₂ (Figure 2b) show no remarkable differences. No noticeable solvatochromic shift is observed for any of the oligomers. For all oligomers, it is worth noting that no

absorption bands are observed in the longer wavelength region (400–600 nm), which would correspond to the charge transition from the electron-rich thiophene unit to the electron-deficient oxadiazole unit. It can be seen from Table 1 that the optical band gap of T₂O₂ is smaller with respect to that of T₂O, indicating a greater delocalization of electronic charge in T₂O₂. In the same way, the relatively smaller band gap of T₄O₂ with respect to T₂O₂ ascribes to two more thiophene rings in T₄O₂ compared with T₂O₂. Interestingly, T₂O₂ has a different optical band gap with its regioisomer OT₂O. The data in Table 1 also reveal that this interesting fact exists between T₄O₂ and its regioisomer T₂O₂T₂. These results confirm that changing the length of the thiophene and oxadiazole units as well as altering the molecular regiochemistry could effectively modulate the band gaps of the oligomers.

Figure 2a,b shows the normalized fluorescence emission spectra of the oligomers in toluene and CH₂Cl₂. All of

(12) (a) Shu, C.-F.; Dodda, R.; Wu, F.-I.; Liu, M. S.; Jen, A. K.-Y. *Macromolecules* **2003**, *36*, 6698. (b) Xu, B.; Pan, Y. C.; Zhang, J. H.; Peng, Z. H. *Synth. Met.* **2000**, *114*, 337. (c) Peng, Z. H.; Zhang, J. H. *J. Chem. Mater.* **1999**, *11*, 1138. (d) Lee, Y.-Z.; Chen, X.; Chen, S.-A.; Wei, P.-K.; Fann, W.-S. *J. Am. Chem. Soc.* **2001**, *123*, 2296.

TABLE 2. Electrochemical Properties and Calculated Energy Differences of the Oligomers

oligomer	reduction ^a	oxidation ^a	LUMO/HOMO ^c (eV)	band gap ^d (eV)
	E_{pa}/E_{pc}^b (V)	E_{pc}/E_{pa}^b (V)		
T₂O	-2.52/-2.36	0.83/0.52	-2.37/-5.37	3.00
T₂O₂	-2.13/-1.99	0.78/0.52	-2.72/-5.39	2.67
T₄O₂	-2.13/-2.03	0.61/0.44	-2.70/-5.15	2.45
OT₂O	-2.51/-2.28	0.76/0.64	-2.40/-5.30	2.90
T₂O₂T₂	-2.32/-2.16	0.83/0.72	-2.60/-5.38	2.78

^a Determined by cyclic voltammetry in CH₂Cl₂ (for oxidation) and THF (for reduction) with Ag/AgNO₃ (0.1 M) as a reference electrode. Scan rate: 200 mVs⁻¹. ^b E_{pa} and E_{pc} stand for anodic peak potential and cathodic peak potential, respectively. ^c HOMO/LUMO = $E_{onset} + 4.7$ eV. ^d Cyclic voltammetric band gap derived from the difference between HOMO and LUMO energy levels.

theoligomers exhibit a notable bathochromic shift (5–20 nm), that is, 18 nm for **T₂O₂** and 20 nm for **T₂O₂T₂**. The solvatochromism may result from an intramolecular charge transfer (ICT) in their excited states.¹³ Two adjacent oxadiazole units have higher electron affinities than the single or isolated oxadiazole unit. Consequently, the ICTs in **T₂O₂** and **T₂O₂T₂** are more effective than those in **T₂O** and **OT₂O**. In the case of diblock oligomers, with the increase in the number of thiophene units in **T₄O₂** relative to **T₂O₂**, the bathochromic shifts result from the formation of a highly extended π -delocalized system.

Figure 3a shows the fluorescence emission spectra of solid thin films on quartz plates prepared by spin coating from solution. Compared to the spectra in CH₂Cl₂ solution, the prominent red shifts (12–34 nm) of emission and (9–32 nm) of absorption (Table 1) are observed for all oligomers. The relatively large Stokes shift reveals that intermolecular association and aggregation exists.

All of the oligomers exhibit only one maximum emission, and this emission maximum was clearly independent of the excitation wavelength. This indicates the existence of an efficient energy transfer from the oxadiazole moiety to the thiophene chromophore.^{9a}

Electrochemical Properties. The redox properties of these materials were determined by cyclic voltammetry in CH₂Cl₂ and THF solutions of 0.1 M tetrabutylammonium hexafluorophosphate (TBAPF₆) using a Pt wire as the counter electrode and a Ag/AgNO₃ (0.1 M) electrode as the reference electrode. The detailed data are listed in Table 2, and the cyclic voltammograms are given in Figure 4. When scanning cathodically, all the oligomers displayed reversible reduction processes. In the case of the diblock oligomers, the increase in the length of the oxadiazole unit changed the reduction potential of those materials remarkably. The reduction potential of **T₂O₂** is shifted by 0.38 V toward less negative values with respect to that of **T₂O** ($E_{T_2O_2}^{1/2(R)} = -2.06$ V¹⁴ and $E_{T_2O}^{1/2(R)} = -2.44$ V vs Ag/Ag⁺; Figure 4a). However, the increase in the thiophene ring number of these materials did not change the reduction potential remarkably. It can be seen from Figure 4b and Table 2 that the addition of one oxadiazole ring from the terminal thiophene side of **T₂O** (**T₂O** → **OT₂O**) had a much smaller effect than the addition of one oxadiazole ring from the terminal oxadiazole

side (**T₂O** → **T₂O₂**) on the reduction potential ($E_{T_2O_2}^{1/2(R)} = -2.06$ V and $E_{OT_2O}^{1/2(R)} = -2.39$ V vs Ag/Ag⁺). This result demonstrates that the molecular regiochemistry can also drastically modulate the reduction potential. This finding also confirms the above hypothesis that strong electronic interaction between two adjacent oxadiazole rings exists. Cyclic voltammetric reduction potential values can be used as a surrogate for LUMO energy levels. The results suggest that the LUMO of those materials can be effectively adjusted by changing the oxadiazole ring number and the molecular regiochemistry.

On sweeping anodically, all of these materials, except **T₂O₂T₂**, undergo a reversible multielectron (two or three) oxidation originating from the thiophene units. Unlike their reduction potentials, the oxidation potentials of diblock oligomers are sensitive to the variation of the thiophene ring number in the thiophene units. The oxidation potential of **T₄O₂** is shifted by 0.13 V toward less positive values with respect to that of **T₂O₂** ($E_{T_2O_2}^{1/2(O)} = 0.65$ V and $E_{T_4O_2}^{1/2(O)} = 0.52$ V vs Ag/Ag⁺; Figure 4c), while the changing of the oxadiazole ring did not change the oxidation potentials remarkably ($E_{T_2O}^{1/2(O)} = 0.66$ V vs Ag/Ag⁺). It is demonstrated that the HOMO level of the diblock oligomers could be effectively adjusted by changing the thiophene number. In the same way, the oxidation potential could be drastically modulated by changing the molecular regiochemistry. Moving the oxadiazole unit of **T₄O₂** into the core of the thiophene unit from the terminal side drastically cut down the oxidation potential ($E_{T_4O_2}^{1/2(O)} = 0.52$ V and $E_{T_2O_2T_2}^{1/2(O)} = 0.77$ V vs Ag/Ag⁺; Figure 4d).

As shown in Table 3, the potential differences between the first and the second oxidation, $\Delta E_p = E_{p1} - E_{p2}$, show remarkable dependence on the molecular regiochemistry and length of the *p*-type unit. **OT₂O** had markedly higher ΔE_p values than its regioisomer **T₂O₂**. Adding an electron-deficient oxadiazole unit to **T₂O** produces a marked increase of ΔE_p , that is, 30 mV between **T₂O** and **T₂O₂** and 220 mV between **T₂O** and **OT₂O**. The difference in the ΔE_p values reflects the Coulombic repulsion (and, hence, the difficulty in stabilizing the dication) between the positive charges in the dicationic state. Therefore, adding an electron-deficient unit to the conjugated oligomer could reduce the Coulombic repulsion effect. Compared with the diblock oligomer **T₂O₂**, the triblock oligomer **OT₂O** showed better delocalization of the positive charges of the dication.

The band gap of the oligomers derives from the difference between the HOMO and the LUMO energy levels. As expected, **T₂O** has the biggest HOMO–LUMO gap of the series. The relatively smaller HOMO–LUMO gap of **T₂O₂** with respect to that of **T₂O** ascribes to the much lower LUMO energy level of **T₂O₂**. **T₄O₂** has the smallest HOMO–LUMO gap of the series as a result of it possessing the highest HOMO energy level. The HOMO–LUMO gap of the triblock oligomers (**OT₂O** and **T₂O₂T₂**), as expected, lies between those of **T₂O** and **T₄O₂**. The reason **T₄O₂** has a larger HOMO–LUMO gap than that of the regioisomer **T₂O₂T₂** is due to the much lower HOMO level of **T₄O₂** with respect to that of **T₂O₂T₂**. In the same way, the higher LUMO level of **T₂O₂** with respect to that of **OT₂O** contributes to the relatively larger HOMO–LUMO gap of **T₂O₂**. However, we find that the band gap of the triblock **T₂O₂T₂** is larger than that of the simple diblock **T₂O₂**. This point is opposite to the known band gap control principle in the *p*–*n* diblock oligomer system.

All oligomers undergo both remarkably reversible oxidation and remarkably reversible reduction processes except **T₂O₂T₂**,

(13) (a) Strehmel, R.; Sarker, A. M.; Malpert, T.-H.; Strehmel, V.; Seifert, H.; Neckers, D. C. *J. Am. Chem. Soc.* **1999**, *121*, 1226. (b) Lu, H. F.; Chan, H. S. O.; Ng, S.-C. *Macromolecules* **2003**, *36*, 1543. (c) Li, L.; Collard, D. M. *Macromolecules* **2005**, *38*, 372.

(14) $E^{1/2(R)}$, $E^{1/2(O)} = (E_{pa} + E_{pc})/2$: half-wave reduction and oxidation potentials.

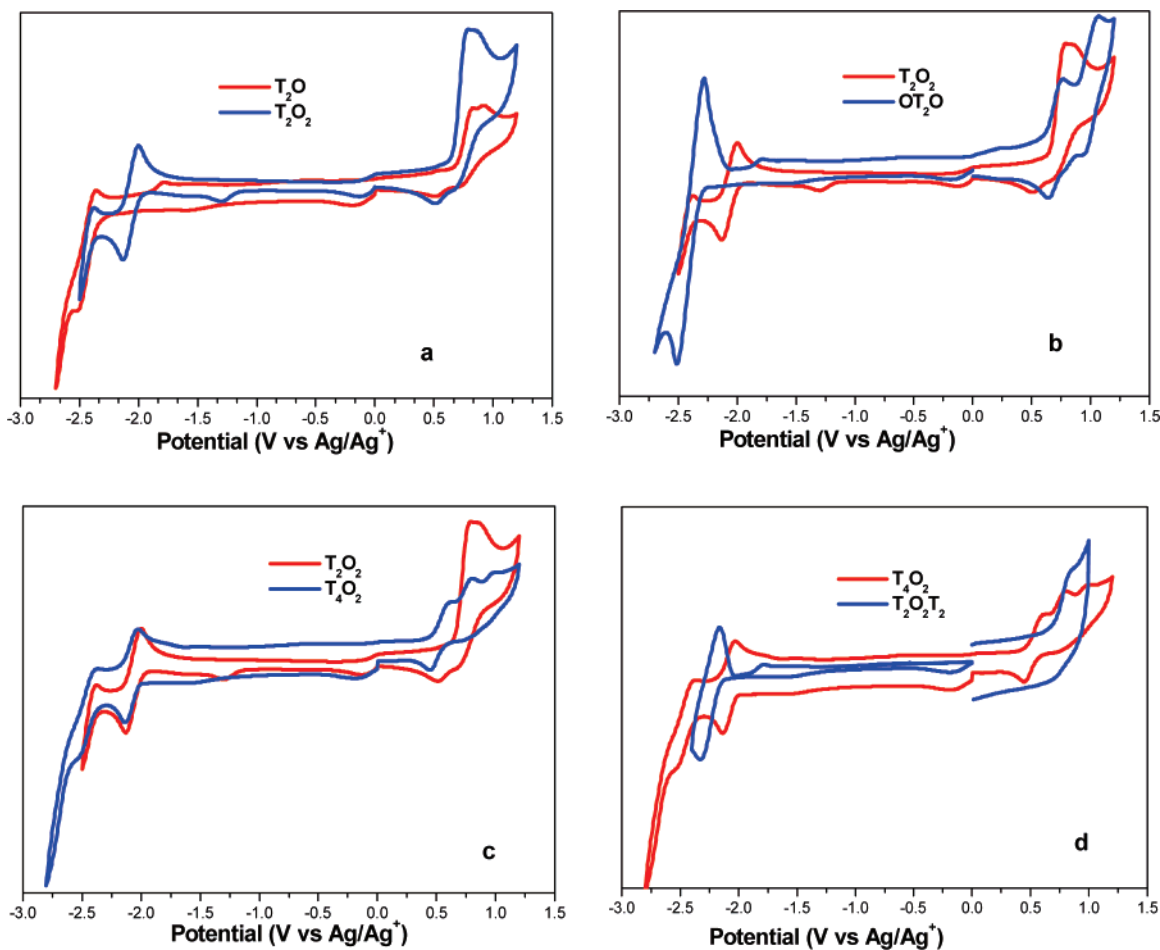


FIGURE 4. Cyclic voltammograms of the oligomers measured in dichloromethane (for oxidation) and THF (for reduction). Scan rate: 200 mVs⁻¹.

suggesting the potential for bipolar charge transport properties.¹⁵ However, most of the respective diblock copolymers show an irreversible oxidation process.³

Theoretical Calculations. The electronic structures of all oligomers were investigated using the density functional theoretical method B3LYP¹⁶ at the 6-31G* basis set calculations of the Gaussian 03 program.¹⁷ The B3LYP functional is a combination of Becke's three-parameter hybrid exchange functional and the Lee–Yang–Parr correlation functional. The alkyl and alkoxy of the molecules were displaced by methyl and methoxy as a result of their minor influence on the electronic and optical properties of the conjugated molecules. The contours of the HOMO and LUMO of the diblock oligomers are plotted in Figure 5. We can see that the HOMO and LUMO of the diblock T_2O are delocalized among the whole molecule. With the increasing number of thiophene or oxadiazole rings of the T_2O_2 and T_4O_2 systems, the HOMO and LUMO tend to be localized on the thiophene and oxadiazole moieties of the systems, respectively. These results demonstrate that the HOMO and LUMO energy levels of T_2O_2 and T_4O_2 can be modulated independently by the thiophene and oxadiazole moieties. However, the HOMO and LUMO of triblock oligomers (OT_2O

and $T_2O_2T_2$) are delocalized to some degree on the whole molecule (see Supporting Information). The trend of the calculated HOMO and LUMO energy levels and the difference (ΔE) between them correlates well with that obtained from the electrochemical measurement and the optical band gap (Table 2). This indicates that our calculation can be used to predict the electronic structures of the system. The calculated HOMO and LUMO levels were gathered in Table 4. Calculated data for the diblock oligomers show that, as expected, the LUMO level decreases with an increase in the length of the oxadiazole unit, and the HOMO level increased with an increase in the length of the thiophene unit.

(15) Li, X.-C.; Liu, Y.; Liu, M. S.; Jen, A. K.-Y. *Chem. Mater.* **1999**, *11*, 1568.

(16) Becke, A. D. *J. Chem. Phys.* **1993**, *98*, 5648. (b) Lee, C.; Yang, W.; Parr, R. G. *Phys. Rev. B: Solid State* **1988**, *37*, 785.

(17) Frisch, M. J.; Trucks, G. W.; Schlegel, H. B.; Scuseria, G. E.; Robb, M. A.; Cheeseman, J. R.; Montgomery, J. A., Jr.; Vreven, T.; Kudin, K. N.; Burant, J. C.; Millam, J. M.; Iyengar, S. S.; Tomasi, J.; Barone, V.; Mennucci, B.; Cossi, M.; Scalmani, G.; Rega, N.; Petersson, G. A.; Nakatsuji, H.; Hada, M.; Ehara, M.; Toyota, K.; Fukuda, R.; Hasegawa, J.; Ishida, M.; Nakajima, T.; Honda, Y.; Kitao, O.; Nakai, H.; Klene, M.; Li, X.; Knox, J. E.; Hratchian, H. P.; Cross, J. B.; Bakken, V.; Adamo, C.; Jaramillo, J.; Gomperts, R.; Stratmann, R. E.; Yazyev, O.; Austin, A. J.; Cammi, R.; Pomelli, C.; Ochterski, J. W.; Ayala, P. Y.; Morokuma, K.; Voth, G. A.; Salvador, P.; Dannenberg, J. J.; Zakrzewski, V. G.; Dapprich, S.; Daniels, A. D.; Strain, M. C.; Farkas, O.; Malick, D. K.; Rabuck, A. D.; Raghavachari, K.; Foresman, J. B.; Ortiz, J. V.; Cui, Q.; Baboul, A. G.; Clifford, S.; Cioslowski, J.; Stefanov, B. B.; Liu, G.; Liashenko, A.; Piskorz, P.; Komaromi, I.; Martin, R. L.; Fox, D. J.; Keith, T.; Al-Laham, M. A.; Peng, C. Y.; Nanayakkara, A.; Challacombe, M.; Gill, P. M. W.; Johnson, B.; Chen, W.; Wong, M. W.; Gonzalez, C.; Pople, J. A. *Gaussian 03*, revision B.04; Gaussian, Inc.: Pittsburgh, PA, 2004.

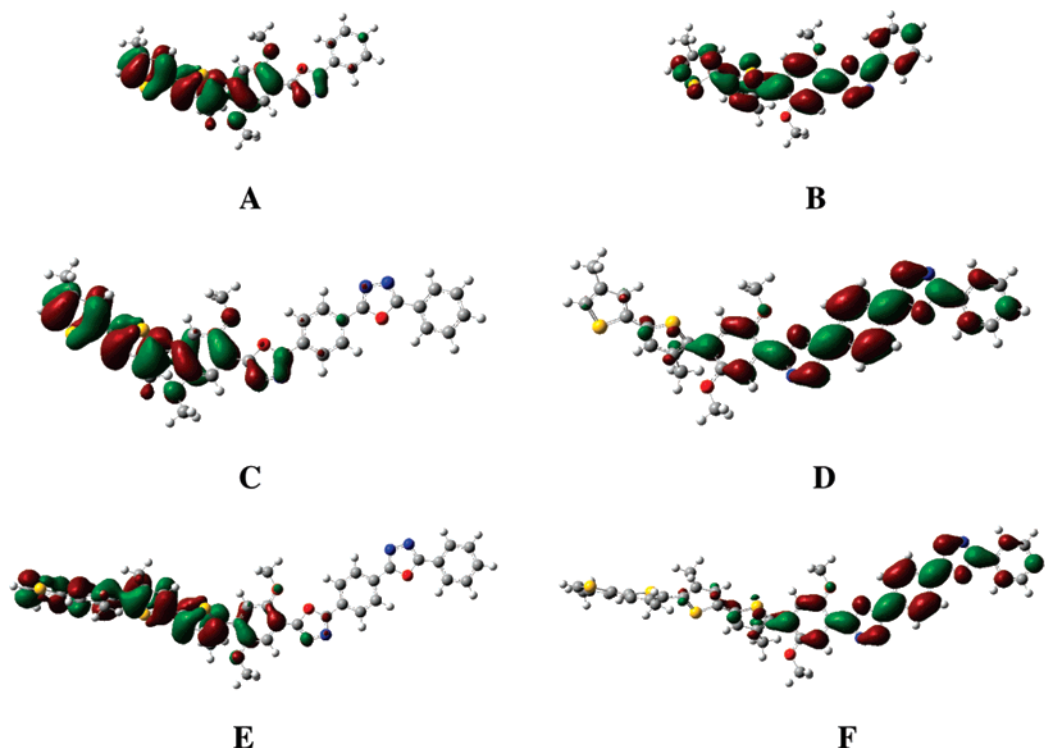


FIGURE 5. Molecular orbital contours of the HOMO (A) and LUMO (B) for the T_2O molecule, the HOMO (C) and LUMO (D) for the T_2O_2 molecule, and the HOMO (E) and LUMO (F) for the T_4O_2 molecule.

TABLE 3. Cyclic Voltammetric Data of Oligomers for Oxidation Potential

oligomer	E_{pl}^a (V)	E_{p2}^a (V)	ΔE_{p} (mV)
T_2O	0.83	0.91	80
T_2O_2	0.78	0.88	100
OT_2O	0.76	1.07	310

^a For the conditions, see Table 2.

TABLE 4. HOMO/LUMO Energy Levels and Gaps^a

oligomer	HOMO (eV)	LUMO (eV)	ΔE (eV)	band gap (eV)	E_{g} (eV)
T_2O	-5.18	-1.69	3.49	3.00	2.98
T_2O_2	-5.23	-2.11	3.12	2.67	2.90
T_4O_2	-5.04	-2.12	2.92	2.45	2.77

^a ΔE calculated by the DFT method (B3LYP/6-31G*).

Conclusions

A new series of p - n diblock and triblock oligomers consisting of an electron-rich thiophene unit and an electron-deficient oxadiazole unit were synthesized and characterized. The p - n diblock oligomers exhibited excellent band-gap controlling properties. Changing the number of the thiophene and oxadiazole rings could effectively modulate the electronic properties of these oligomers. Density functional theory provided evidence for the observed electronic properties. In comparison with

triblock oligomers, the HOMO and LUMO energy levels of the p - n diblock oligomers completely localized on the thiophene and oxadiazole unit, respectively. Changing the thiophene or oxadiazole ring number could independently tune the HOMO or LUMO energy level in the p - n diblock oligomers. Thus, the diblock oligomers were more effectively adjusted in regard to their HOMO/LUMO energy levels than the triblock oligomers. Additionally, the electronic properties could be drastically modulated by molecular regiochemistry. The study, therefore, provided fundamental insight into the improved design and understanding of p - n heterostructure oligomer semiconductors.

Acknowledgment. This work was financially supported by the National Natural Science Foundation of China under Grants 60325412 and 90406021, the Shanghai Commission of Science and Technology under Grants 03DZ11016 and 04XD14002, and the Shanghai Commission of Education under Grant 03SG03. We would also like to thank Professor Z. M. Su and Dr. G. C. Yang, Northeast Normal University, for their helpful discussion about theoretical calculations.

Supporting Information Available: Detailed synthetic procedures, ^1H and ^{13}C NMR spectra for all oligomers, molecular orbital contours of the HOMO and LUMO for OT_2O and $\text{T}_2\text{O}_2\text{T}_2$, and a table of atom coordinates used in the calculations. This material is available free of charge via the Internet at <http://pubs.acs.org>.

JO0521596